O-7-1
Extended Abstracts of the 2015 International Conference on Solid State Devices and Materials, Sapporo, 2015, pp1194-1195

Low power switching of Si-doped Ta_2O_5 ReRAM for high density memory application

Beom Yong Kim, Kee Jeung Lee, Su Ock Chung, Soo Gil Kim, and Hyeong Soo Kim

New Memory Process Group, R&D division SK hynix Semiconductor Inc.,
San136-1, Ami-ri, Bubal-eub, Icheon-si, Gyeonggi-do, 467-701, Korea
Phone: +81-31-639-4386 E-mail: beomyong2.kim@sk.com

Abstract

We report, for the first time, the resistive switching properties of Si-doped Ta_2O_5 grown by atomic layer deposition. The low power operation is successfully demonstrated in the Si-doped Ta_2O_5 ReRAM devices of 50nm tech node. The switching mechanism for the Si-doped Ta_2O_5 resistor is discussed. Si dopants enable a switching layer to have conformal distribution of oxygen vacancy and easily form conductive filament.

1. Introduction

In order to be more competitive for high density memory application, ReRAM cells are required to low operation current below 10μA [1]. Ta_2O_5 is the widely used material for ReRAM due to its good endurance [2-3]. However, the operation current is still high level (50-100μA). Recently, it is reported that the good switching performance was obtained using defect engineering such as oxygen reduction or impurity implantation [4-5]. However, these defect engineering technologies may have fundamental limitations for application of multi-plane and 3D vertical type structures. Thus, the defect engineering process during the film deposition is much more desirable. We predict that silicon doping would be advantageous to oxygen vacancy (V_o) formation in Ta_2O_5 film because of the chemical valence difference between Ta^{5+} and Si^{4+} [5]. In this study, we demonstrated the switching properties of Si-doped Ta_2O_5 using atomic layer deposition (ALD). Moreover, oxygen reduction of Ta_2O_5 by hydrogen plasma treatment (HP) was conducted as a comparison.

2. Device Fabrication and experiment

The amount of Si doping in Ta_2O_5 is controlled by the ratio of Ta_2O_5 and SiO_2 ALD subcycles (Fig. 1). Fig. 2 shows the process flow of the fabricated ReRAM structure with 50nm tech node. Ti_4O_7 is taken for a reservoir layer. Ta_2O_5 reduced by hydrogen plasma treatment (Ta_2O_5-HP) was also formed to compare with Si-doped Ta_2O_5.

3. Results and discussion

Table I shows the composition of Si-doped Ta_2O_5 with Ta_2O_5/SiO_2 subcycle ratios. Fig. 3(a) shows XPS Ta5f spectra. In case of Ta_2O_5-HP, the surface of Ta_2O_5 was reduced. However, there are no noticeable changes in Si-doped Ta_2O_5 with the increase of Si doping concentration. On the other hand, for Si2p XPS spectra as shown in Fig. 3(b), SiO_x was formed and the peak intensity of SiO_x increased as the increase of Si content. This result in turn confirms the idea that oxygen vacancies can be generated by utilizing ALD SiO_2 and Ta_2O_5 subcycles. Thermodynamic approach explains that Ta could consume oxygen from SiO_2 and therefore form SiO_x having V_o (Eq. (1), (2)).

DC I-V switching characteristics as a function of compliance current (CC) were measured for the Ta_2O_5-HP and Si-doped (2.4% atomic percent) Ta_2O_5 resistor stacks. In case of Ta_2O_5-HP, on/off current ratio (I_{on}/I_{off}) of 4.4 was achieved at 20μA CC but resistive switching did not occur at lower CC, 5μA (Fig. 4). Surprisingly, Si-doped Ta_2O_5 stack shows the improved switching (I_{on}/I_{off} >5) not only at 20μA CC but also at 5μA CC (Fig. 5-6). In addition, the endurance property was not degraded up to 80000 cycles, as shown in Fig. 7.

From linear fitting of high resistance state (HRS), Si-doped Ta_2O_5 shows the better linearity of Poole-Frenkel emission fitting than Ta_2O_5-HP (Fig. 8, 9). Moreover, Si-doped Ta_2O_5 has higher low resistance state (LRS) current than Ta_2O_5-HP, while there is little difference in HRS currents (Fig. 10). This indicates that a conductive filament in Si-doped Ta_2O_5 film is easily formed during set-process. In case of Ta_2O_5-HP stack, it is difficult to form filament due to insufficient V_o drift energy at low operation current (CC <20μA) (Fig. 11(a)). On the other hand, for Si-doped Ta_2O_5 stack, V_o migrates not only from Ti_4O_7 but also from Si-doped Ta_2O_5 because V_o may uniformly distribute in the Si-doped Ta_2O_5 films (Fig. 11(b)). Thus, Si-doped Ta_2O_5 could form filament and increase on/off current ratio at even low current.

4. Conclusion

We reported, for the first time, the switching behaviors of Si-doped Ta_2O_5 ReRAM grown by ALD. It exhibited low power switching (I_{on}/I_{off} >5 at 5μA CC) and good endurance (>8000cycles). Systematic analysis clearly explains the switching mechanism of Si-doped Ta_2O_5 that the conformal distribution of V_o in Si-doped Ta_2O_5 film allows a boost in on/off ratio and operation current scaling, which makes this ALD Si-doped Ta_2O_5 promising for future high density and 3D type ReRAM applications.

References

[1] B. Govoreanu et al., IEDM Tech. Dig., pp 10.2.1, (2013)
[2] Z. Wei et al., IEDM Tech. Dig., pp 1, (2008)
[3] B. Y. Kim et al., Jpn. J. Appl. Phys. 52 04CD05 (2013)
[4] Y.Y. Chen et al., IEEE Electron Device Lett. Vol. 33, pp 483 (2012)
[5] H. Zhang et al,. Appl. Phys. Lett. 96, 123502 (2010)

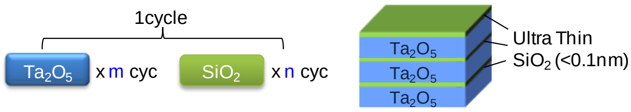

Fig. 1. ALD process consisting of Ta_2O_5 and SiO_2 subcycles

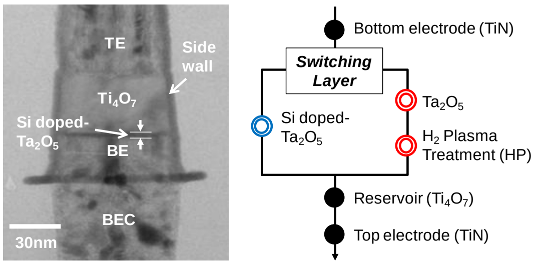

Fig. 2. (a) Crosssection TEM image of the fabricated ReRAM structure and (b) process flow. The bottom electrode contact (BEC) size is 50 nm

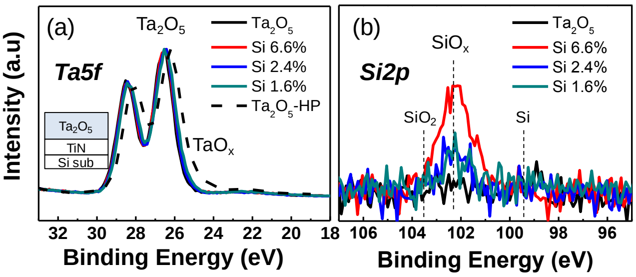

Fig. 3. XPS spectra of Ta_2O_5, Si-doped Ta_2O_5, and Ta_2O_5-HP. (a) Ta 5f, (b) Si 2p.

$$Si+O_2=SiO_2,\ \triangle G^0 = -190.8kcal/mol \quad (1)$$

$$4/5Ta+O_2=2/5Ta_2O_5,\ \triangle G^0 = -339.8kcal/mol \quad (2)$$

TABLE I. The composition of Si doped Ta_2O_5 with Ta_2O_5 and SiO_2 subcycle ratio.

TaO/SiO Cycle Ratio	Atomic percent (%)		
	O	Si	Ta
2:1	71.9	6.6	21.5
5:1	73.1	2.4	24.5
8:1	72.9	1.6	25.5

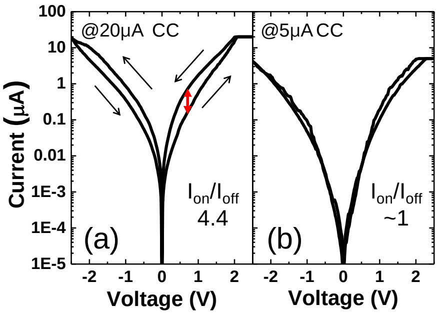

Fig. 4. The switching results after the fifth I-V sweeps for Ta_2O_5-HP with compliance current (CC). (a) 20μA CC, (b) 5μA CC. On/off current ratio was measured at 0.7V.

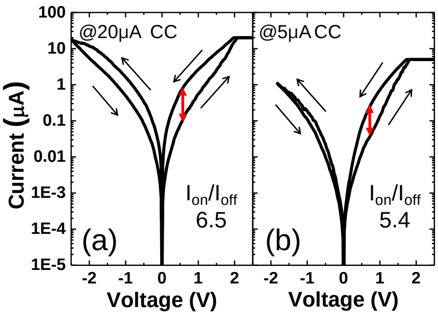

Fig. 5. The switching results after the fifth I-V sweeps for Si-doped (2.4% atomic percent) Ta_2O_5 with CC. (a) 20μA CC, (b) 5μA CC.

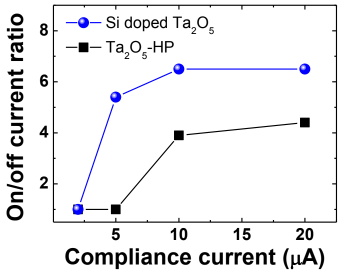

Fig. 6. On/off current ratios as a function of CC for Si-doped Ta_2O_5 and Ta_2O_5-HP cells.

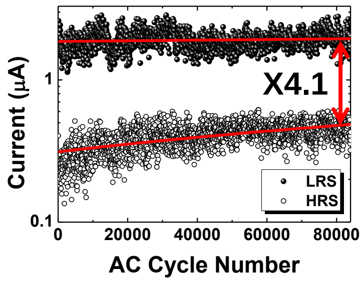

Fig. 7. AC endurance characteristics of Si-doped Ta_2O_5 stack.

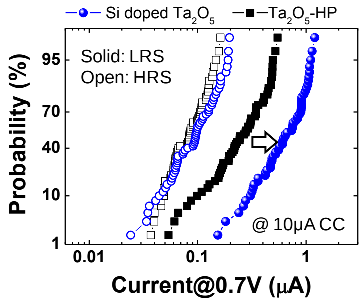

Fig. 10. HRS and LRS currents of Si doped Ta_2O_5 and Ta_2O_5-HP cells.

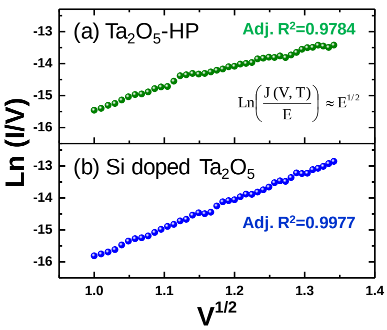

Fig. 8. Linear fitting of HRS from 5[th] cycle of switching I-V. (a) Ta_2O_5-HP, (b) Si doped Ta_2O_5.

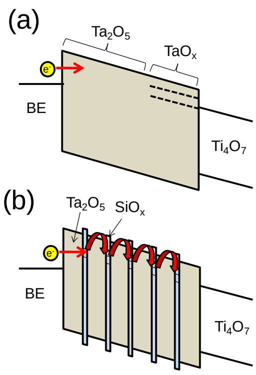

Fig. 9. Schematic band diagrams of (a) Ta_2O_5-HP and (b) Si-doped Ta_2O_5 stack in HRS.

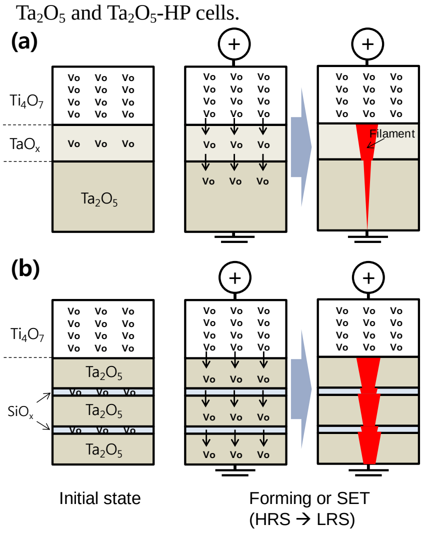

Fig. 11. Switching mechanism (a) Ta_2O_5-HP resistor, (b) Si doped Ta_2O_5 resistor.